Multi-functional liposomes having temperature-triggered release and magnetic resonance imaging for tumor-specific chemotherapy

Multi-functional liposomes having temperature-triggered release and magnetic resonance imaging for tumor-specific chemotherapy

Kenji Kono[1,*], Seiji Nakashima[1], Daisuke Kokuryo[2], Ichio Aoki[2], Hiroaki Shimomoto[3], Sadahito Aoshima[3], Kazuo Maruyama[4], Eiji Yuba[1], Chie Kojima[5], Atsushi Harada[1] and Yukihito Ishizaka[6]

[1]Department of Applied Chemistry, Graduate School of Engineering,

Osaka Prefecture University

1-1, Gakuen-cho, Sakai, Osaka 599-8531, Japan

[2] Molecular Imaging Center, National Institute of Radiological Sciences

4-9-1, Anagawa, Inage-ku, Chiba-shi, 263-8555, Japan

[3]Department of Macromolecular Science, Graduate School of Science,

Osaka University,

Toyonaka, Osaka 560-0043, Japan

[4]Department of Pharmaceutical Sciences

Teikyo University

Sagamiko, Sagamihara, Kanagawa 229-0195, Japan

[5]Nanoscience and Nanotechnology Research Center, Research Organization for the 21st Century, Osaka Prefecture University, 1-2 Gakuen-cho, Naka-ku, Sakai, Osaka 599-8570, Japan

[6]Department of Intractable Diseases

Research Institute, International Medical Center of Japan

1-21-1 Toyama, Shinjuku-ku, Tokyo 162-8655, Japan

***Corresponding author: Kenji Kono**

Department of Applied Chemistry, Graduate School of Engineering, Osaka Prefecture University

1-1, Gakuen-cho, Naka-ku, Sakai, Osaka 599-8531, Japan

Tel: +81-72-254-9330; Fax: +81-72-254-9330; E-mail: kono@chem.osakafu-u.ac.jp

KEYWORDS: drug delivery, temperature-responsive, doxorubicin, chemotherapy, thermosensitive polymer, MRI

Abstract

Toward development of tumor-specific chemotherapy, we designed a new type of liposomes with temperature-triggered drug release and magnetic resonance imaging (MRI) functions. We prepared the multi-functional liposomes by incorporation of thermosensitive poly(2-ethoxy(ethoxyethyl) vinylether) chains with a lower critical solution temperature around 40°C and polyamidoamine G3 dendron-based lipids having Gd^{3+} chelate residues into pegylated liposomes. The liposomes loaded with doxorubicin (DOX) were stable and retain DOX in the interior below physiological temperature but released DOX immediately above 40°C. In addition, the liposomes exhibited an excellent ability to shorten the longitudinal proton relaxation time. When administered intravenously into colon 26 tumor-bearing mice, accumulation of the liposomes in tumors was shown to increase with time and to reach to a constant level 8 h after the administration by following T_1-weighted MRI signal intensity in tumors. The efficiency of the liposome accumulation in tumor was affected by liposome size; the liposomes with a diameter of about 100 nm were more efficiently accumulated in tumor than those with a diameter of about 50 nm. The liposomes accumulation was also affected by tumor size and exhibited more efficient accumulation in the larger tumor. When the liposomes loaded with DOX were administered intravenously into tumor-bearing mouse and tumor was mildly heated at 44^{o}C for 10 min at 8 h after administration, tumor growth was strongly suppressed thereafter. The multi-functional liposomes having temperature-triggered drug release and MRI functions may lead to personalized chemotherapy, which provides an

efficient chemotherapy optimized to each patient.

1. Introduction

Toward establishment of safe and effective tumor therapy, accurate drug delivery is a promising approach, which enables to attack specifically the target malignant cells with drugs [1-3]. Regarding improvement of tumor specificity of drug delivery, efficient strategies are the use of nano-sized particles with a long circulation property with stimuli-sensitive properties as drug carriers. The former can improve accumulation of the carriers in tumor tissues through the enhanced permeation and retention (EPR) effect [4,5] and the latter can increase therapeutic effect by releasing drug specifically at the diseased tissues upon application of stimuli to the target sites [6-8]. In addition, another important function for the improvement of accuracy of drug delivery might be imaging function of carriers [9-14]. If drug carriers have these functions and properties, efficient cancer chemotherapy can be achieved by following accumulation of carriers to the target sites and triggering drugs by stimuli application after the maximum acculturation of the carriers at the targets sites. In addition, accumulation process of the carriers should vary depending on individual patient. Therefore, carriers with these functions should lead to personalized chemotherapy, which is optimized to each patient.

Recently, efforts have been made to provide imaging functions to various types of carriers by incorporating various types of imaging probes, such as quantum dots [15-17],

magnetic iron oxide nanoparticles [11,12,18,] and radionuclide ^{18}F [19,20] have been incorporated to drug carrier materials for fluorescence imaging, magnetic resonance imaging (MRI), and positron emission tomography (PET) imaging, respectively. Among them, MRI is advantageous from the view points of image of high resolution and no exposure to radiation. Also, MRI has no time limit for detection in contrast to PET with ^{18}F whose half-life is 109.8 min. Therefore, MRI is one of the best methods for visualization of drug delivery systems in the body from the practical sense.

Among various types of drug delivery systems, liposomes are of importance as drug delivery vehicle from the viewpoints of biodegradability, size-controllability and high drug encapsulation ability. In addition, stimuli-responsive functions can be provided to liposomes by using temperature-induced phase transition of the liposome membranes [21-24] or incorporating temperature-sensitive polymers into the liposome membrane [25-31].

Based on these advantages of liposomes, many attempts have been made to provide MR imaging functions to them [14]. Considering that the liposome lumen must be used to encapsulate large amounts of drug molecules, the membrane moiety might be suitable for the incorporation of MRI probes. Therefore, lipid-based MRI contrast agents, such as amphiphilic Gd-DTPA derivatives [32,33] have been used for this purpose. Because these molecules contain single Gd-chelate moiety per molecule, inclusion of a high content of these amphiphilic Gd-chelate molecules might be necessary in the liposomes to gain high detectability with MRI, which should affect performance of the liposomes. Also,

macromolecular Gd-chelates, which have several Gd-chelate residues in the single molecular chain, have been incorporated to liposomes [13,34,35]. However, incorporation of such macromolecular polychelates taking on a extended structure may affect surface property of the liposomes.

In order to obtain multi-functional liposomes which exhibit both highly stimuli-responsive drug release and highly detectable MR imaging functions, we designed biocompatible pegylated liposomes having both highly thermosensitive polymers and amphiphilic poly(Gd-chelates) with a compact conformation. For this purpose, in this study, we newly synthesized polyamidoamine (PAMAM) G3 dendron-based lipids having eight Gd^{3+} chelate residues (G3-DL-DOTA-Gd). Because of the highly branched backbone structure with many chain terminals, the dendron moiety taking on a compact conformation can hold many Gd-chelate residues. Based on the highly temperature-responsive liposomes, which were developed recently by modification of pegylated liposomes with thermosensitive poly [2-(2-ethoxy)ethoxyethyl vinyl ether-*block*-octadecyl vinyl ether (EOEOVE-*block*-ODVE)] with a lower critical solution temperature (LCST) around 40°C [36,37], we incorporated the dendron-based lipid having many Gd-chelates into the poly(EOEOVE-*block*-ODVE)-modified liposomes (Figure 1). Performances of the liposomes from the sense of visualization and tumor-chemotherapy were investigated. Importance of the visualization of accumulation process of the liposomes at the tumor sites and the heat-triggered drug release function of the liposome to achieve a highly reliable and efficient

chemotherapy was described.

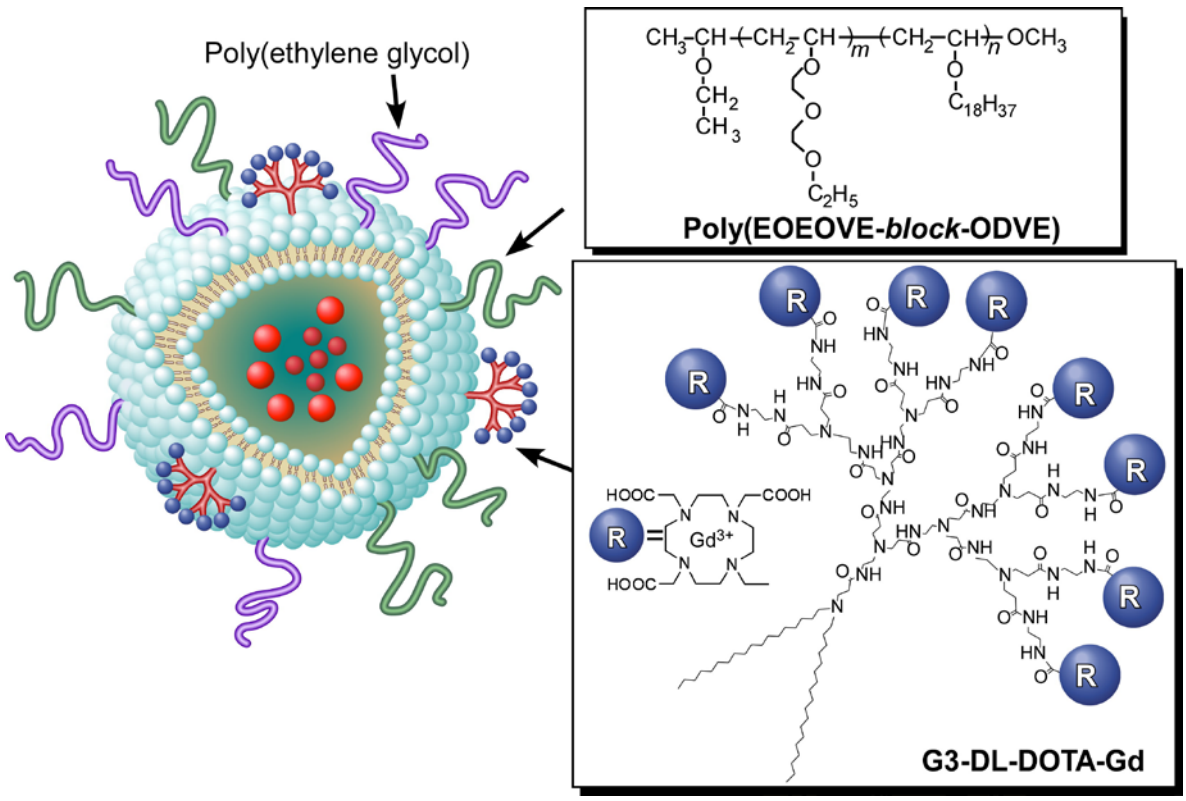

Figure 1. Schematic illustration of design of functional liposome having temperature-controlled drug release and MR detection functions. Chemical structures of poly(EOEOVE-*block*-ODVE) and G3-DL-DOTA-Gd were shown in the figure.

2. Materials and Methods

2.1. Materials

Egg yolk phosphatidylcholine (EYPC) and N-[methoxy (polyethylene glycol) 5000 or 2000]-distearoyl phosphatidylethanolamine (PEG-PE) were kindly donated by Nippon Oil and Fats Co. (Tokyo, Japan). Doxorubicin (DOX) was kindly donated by Kyowa Hakko Kirin Co. Ltd. (Tokyo, Japan). 1,4,7,10-Tetraazacyclododecane-1,4,7,10-tetraacetic acid mono(N-

hydroxysuccinimidyl ester)（DOTA-NHS）and fluorescamine were provided from Tokyo Kasei Kogyo (Tokyo, Japan). Cholesterol (Chol) was obtained from Sigma (St. Louis, MO.). PAMAM G1 and G3 dendron-based lipids (G1-DL and G3-DL) were synthesized as reported previously [38]. Copoly[EOEOVE-*block*-octadecyl vinylether(ODVE)] was synthesized as previously reported using 1-(ethoxy)ethyl acetate as the initiator [36]. The number average molecular weight and polydispersity index of copoly(EOEOVE-*block*-ODVE) were estimated to be $1.3x10^4$ and 1.03, respectively, using gel permeation chromatograpy. The number average molecular weights of poly(EOEOVE) block and poly(ODVE) block were estimated to be 87 and 7, respectively, using ^{1}H NMR. The copolymer was shown to undergo a transition between 36 and 46 °C with a peak at 38.2°C using DSC.

2.2. Animals

Female BALB/c mice were purchased from Oriental Yeast Co., Ltd. (Tokyo, Japan) and Japan SLC, Inc. (Shizuoka, Japan). Experiments were carried out in accordance with the guidelines for animal experimentation in Osaka Prefecture University and National Institute of Radiological Sciences.

2.3. Synthesis of G3-DL-DOTA and G1-DL-DOTA

G3-DL-DOTA was synthesized as follows. G3-DL (105 mg, 47.0 μmol) and triethylamine (678 μL) were dissolved in dimethysulfoxide (5 mL) and added to DOTA-NHS (481 mg, 959 μmol) dissolved in dimethysulfoxide (40 mL). The mixed solution was stirred at room temperature for 4 days under an argon atmosphere until the reaction was completed using

ninhydrin test. Then, the compound was purified by dialysis against distilled water using a Spectra/Por® dialysis membrane (MWCO:1000Da) and obtained by freeze-drying. Yield: 182 mg. G1-DL-DOTA was synthesized by the same method using G1-DL (105 mg). Yield: 141 mg.

2.4. Preparation of G3-DL-DOTA-Gd and G1-DL-DOTA-Gd

G3-DL-DOTA-Gd was prepared by chelate formation between G3-DL-DOTA and Gd^{3+}. Typical procedure was as follows. G3-DL-DOTA (72.4 mg, 14.9 μmol) was dissolved in water (10 mL) and the solution was added to $GdCl_3$ (314 mg, 1.19 mmol) dissolved in water. The pH of the mixed solution was adjusted to be 7.3 with an aliquot of NaOH solution and sonicated at 50 ºC for 150 min under an argon atmosphere using a bath-type sonicator. Then, the G3-DL-DOTA-Gd was purified by dialysis against distilled water using a Spectra/Por® dialysis membrane (MWCO:1000Da) and subsequent centrifugation at 15000 rpm for 2 h, and then recovered by freeze-drying. Yield: 141 mg. G1-DL-DOTA-Gd was prepared by the same procedure by chelate formation between G1-DL-DOTA and Gd^{3+}.

2.5. Preparation of liposomes

Liposomes were prepared according to the method previously reported [37]. A thin dry membrane of a mixture of EYPC, Chol, copoly(EOEOVE-*block*-ODVE), and PEG-PE and G3-DL-DOTA-Gd at the molar ratio of 42/42/4/2/5-10 was dispersed in 20 mM Hepes and 150 mM NaCl solution of pH7.4 (HBS, 1 ml) by brief sonication using a bath-type sonicator. Then, the obtained liposome suspension was extruded through a polycarbonate membrane

with a pore size of 50 or 100 nm and purified by dialysis in HBS. For preparation of DOX-loaded liposomes, the EYPC, Chol, copoly(EOEOVE-*block*-ODVE), and PEG-PE and G3-DL-DOTA-Gd was dispersed in 300mM ammonium sulfate (pH 5.3) by hydrated by brief sonication using a bath-type sonicator. The obtained liposome suspension was extruded through a polycarbonate membrane with a pore diameter of 100 nm and was dialyzed in HBS for formation of pH gradient. Then aqueous DOX solution (10 mg/ml) was added to the liposome suspension at DOX/lipid (g/mol) ratio of 100 and the mixed solution was incubated for 1 h at 30 ºC. Free DOX was removed from the liposome suspension by using a Sepharose 4B column with HBS and the DOX-loaded liposome suspension was kept at 4 ºC until the measurements. EYPC concentration was determined using Phospholipid C Test Wako (Wako Pure Chemical Industries Co., Ltd., Osaka, Japan). Encapsulation efficiency of DOX by liposomes was estimated from absorbance of DOX at 499 nm for the DOX-loaded liposomes dissolved in 0.3 N HCl (50vol%)-ethanol (50 vol%) before and after purification with a Sepharose 4B column [24].

2.5. DOX release from liposomes

The release measurements were performed according to the method previously reported [37]. An aliquot of dispersion of the DOX-loaded liposomes was added into 3 ml of HBS in a quartz cell (final concentration of the lipids 13.3 μM) at a given temperature and the fluorescence intensity of the solution was monitored using a spectrofluorometer (JASCO FP-6200ST). The excitation and monitoring wavelengths were 468 nm and 590 nm,

respectively. The percent release of DOX from liposomes was defined as

% release = $(F^t - F^i)/(F^f - F^i) \times 100$

where F^t and F^f are intermediary and final fluorescence intensities of the vesicle suspension at a given temperature. F^f was obtained as the fluorescent intensity of the liposome suspension after rupture of liposomes was induced by the addition of 10 % Triton X-100 solution (30μl). Because DOX was released very quickly above 40 ºC, it was difficult to estimate initial fluorescence intensity of the DOX-loaded liposome suspension. We took the initial fluorescence intensity of the suspension at 10 ºC, where release of DOX was negligible and DOX fluorescence was strongly quenched.

2.6. Relaxivity

The T_1 of Gd (0-1.14 mM) for Gd-DOTA-containing molecules and liposomes in HBS were evaluated using a 7T MR scanner (magnet: Kobelco and Jastec, Japan, Console: Bruker-Biospin, Germany) using the following imaging sequence and parameters: 2D single-slice fast spin-echo sequence (rapid acquisition with relaxation enhancement) with inversion recovery, echo time (TE)=9.60 ms, repetition time (TR)=10000 ms, inversion time=50.5, 100, 200, 400, 800, 1600, 3200 and 6400 ms, field of view (FOV) = 51.2 x 51.2 mm^2, slice thickness=2.0 mm, and RARE factor=4.

2.7. In Vivo MR imaging

Tumor-bearing mice were prepared by inoculating mouse colon carcinoma 26 cells ($1x10^6$ cells) into both upper hind legs of BALB/c nude mice (9-12 weeks old, female) under

anesthesia and the tumor was allowed to grow for about 10 days. For preparation of mice with different tumor sizes, the cells ($4x10^6$ cells) were additionally inoculated into the upper hind of right leg. The G3-DL-DOTA-Gd-incorporated liposomes consisting of EYPC, Chol, copoly(EOEOVE-*block*-ODVE), and PEG-PE and G3-DL-DOTA-Gd at the molar ratio of 42/42/4/2/10 (2.96 μmol lipid) were injected via the tail vein into tumor-bearing mice. Contrast-enhanced T_1-weighted images of mice were taken with the 7T MR scanner using the following imaging sequence and parameters: TE=9.57 ms, TR=300 ms, FOV=44.8 x 44.8 mm^2, slice thickness=1.0 mm, and number of aquesition=4.

2.8. Anti-tumor effect of DOX-loaded liposomes

Anti-tumor effect of DOX-loaded liposomes was examined as previously reported [37,39]. Tumor-bearing mice were prepared by inoculating mouse colon carcinoma 26 cells ($1x10^6$ cells) into the right flank of BALB/c mice (female, 5-6 weeks old) under anesthesia and the tumor was allowed to grow for about 10 days, when the volume was approximately 200 mm^3. DOX-loaded liposomes were injected intravenously at a dose of 6 mg/kg via the tail vein under anesthesia. At 8 h after the injection, tumor was locally heated at 44 ºC for 10 min using a radiofrequency oscillator (RF-hyperthermia HEH-100, Omron, Kyoto). Tumor volumes were determined as

$$\text{Volume} = LxW^2/2$$

Where L is the longest dimension parallel to the skin surface and W is the dimension perpendicular to L and parallel to the surface.

2.9. Other methods

Differential scanning calorimetry (DSC) was performed with a DSC 120 microcalorimeter (Seiko Electronics). The size of liposomes was evaluated by dynamic light scattering using an Nicomp 380 ZLS instrument (Particle Sizing System, Santa Barbara, CA). Coupled plasma optical emission spectroscopy measurement was performed using SPS7800 (Seiko Instruments Inc.)

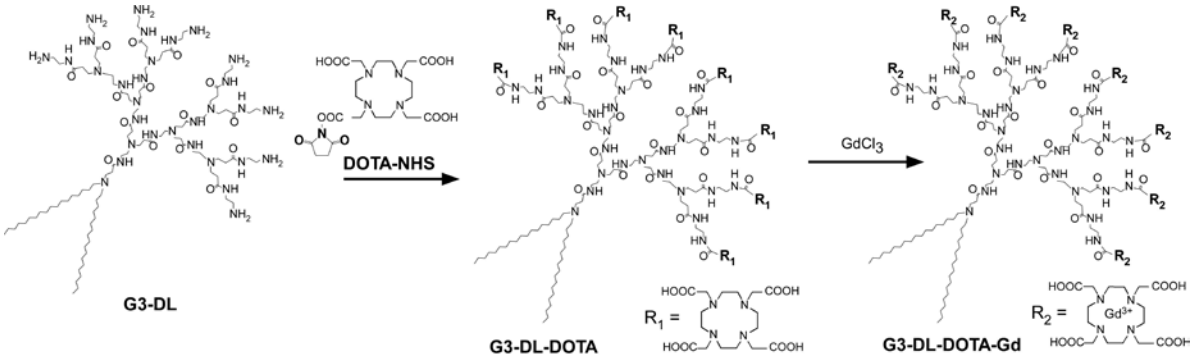

Figure 2. Synthetic route for G3-DL-DOTA-Gd.

3. Results and discussion

3.1. Preparation of dendron-based lipid having Gd chelates

We prepared the dendron-based lipid, G3-DL-DOTA-Gd, according to Figure 2. First, PAMAM G3-DL was reacted with 20 eq. of DOTA-NHS, which corresponds to 2.5 eq. of DOTA-NHS per terminal primary amine of the dendron moiety to obtain G3-DL-DOTA. ^{1}H NMR spectra of DOTA, G3-DL, and G3-DL-DOTA were shown in Figure 3. The NMR

spectrum of obtained G3-DL-DOTA contained peaks around 0.9-1.4 ppm and 3.3 ppm, which are derived from G3-DL, and a peak around 3.1 ppm, which is derived from DOTA, indicating that the obtained G3-DL-DOTA actually consisted of G3-DL and DOTA moieties. However, significant overlap of peaks derived from both G3-DL and DOTA abound 2.2-3.0 ppm made accurate determination of the number of the incorporated DOTA per G3-DL difficult, although it was evaluated to be 7.0 from the integration of these peaks. We further tried to estimate the number of DOTA residues in G3-DL-DOTA by evaluating the number of the residual primary amine groups. T he fluorescamine assay [40] revealed that the number of primary amines remaining in G3-DL-DOTA molecule was estimated to be 0.12 using a calibration curve made with G3-DL as the standard. This result suggests that essentially every chain terminal of the dendron moiety was combined with DOTA residue in G3-DL-DOTA. In the same way, the numbers of residual primary amines were 0.13, indicating that essentially every chain end was connected to DOTA residue in G1-DL-DOTA. These DOTA-incorporated dendron-based lipids were incubated with Gd^{3+} for their chelate formation. The numbers of Gd^{3+} in G3-DL-DOTA-Gd and G1-DL-DOTA-Gd were 7.8 and 1.6, respectively, using inductively coupled plasma optical emission spectroscopy.

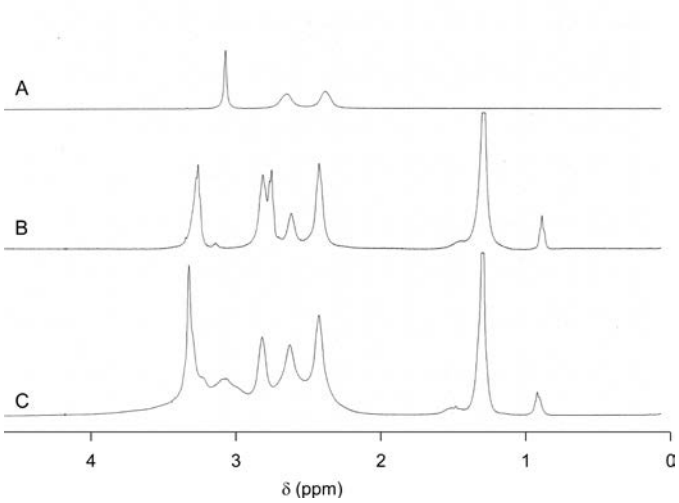

Figure 3. H NMR spectra of DOTA (A), G3-DL (B) and DOTA-G3-DL (C) in D_2O with NaOD.

3.2. Relaxivity of copoly(EOEOVE-block-ODVE)-modified liposomes containing Gd-DOTA-dendron-based lipids

We recently showed that incorporation of copoly(EOEOVE-block-ODVE) to pegylated EYPC/Chol liposomes generates highly temperature-sensitive liposomes, which release encapsulated DOX immediately responding to mild heating [37]. Based on this result, we attempted to prepare multifunctional liposomes by incorporation of Gd-DOTA-dendron-based lipids into the copolymer-modified pegylated liposomes. The potency of MRI contrast agents depends on their ability to shorten the T_1 and T_2 relaxation times of water. The Gd^{3+} ions are known to shorten T_1 relaxation time efficiently and hence their chelates have been used as the so-called T_1-agents for contrast-enhanced T_1-weighted imaging [2]. For highly sensitive detection of liposomes containing the Gd-DOTA-dendron-based lipids in the body, these liposomes must exhibit a high ability to shorten T_1 relaxation time, which is expressed longitudinal relaxivity r_1. Therefore, we evaluated the r_1 values of Gd-DOTA-dendron-based

lipids and their incorporated liposomes. Figure 4 depicts the plots of $1/T_1$ for G1-DL-DOTA-Gd, G3-DL-DOTA-Gd and G3-DL-DOTA-Gd-containing liposomes as a function of Gd^{3+} concentration, which exhibited their linear relationship. Their r_1 values were estimated from the slopes of these lines to be 4.6, 6.2, and 5.5 $mM^{-1}s^{-1}$ for G1-DL-DOTA-Gd, G3-DL-DOTA-Gd and G3-DL-DOTA-Gd-containing liposomes. The r_1 of free Gd-DOTA was also evaluated to be 4.6 $mM^{-1}s^{-1}$. Although the attachment of Gd-DOTA to G1 dendron moiety of the dendron-based lipid did not affect its ability to shorten T_1, its attachment to G3 dendron moiety increased the potency of Gd-DOTA to some extent. It was reported that the r_1 for Gd-DOTA-conjugated PAMAM dendrimers increased with the dendrimer generation, because of the increase of rotational correlation time of the whole molecule, which increases with the molecular weight, and limited internal rotational motions of Gd-DOTA moieties connected to the rather rigid backbone of the dendrimer [41]. Therefore, it is likely that the Gd-DOTA residues attached to larger G3 dendron with highly crowded chain terminals might decrease their mobility and increase their rotational correlation time, resulting in higher relaxivity of the G3-DL-DOTA-Gd than G1-DL-DOTA-Gd. In addition, G3-DL-DOTA-Gd retained the high relaxivity when incorporated into the liposomes, suggesting their high detectability in the body with MRI.

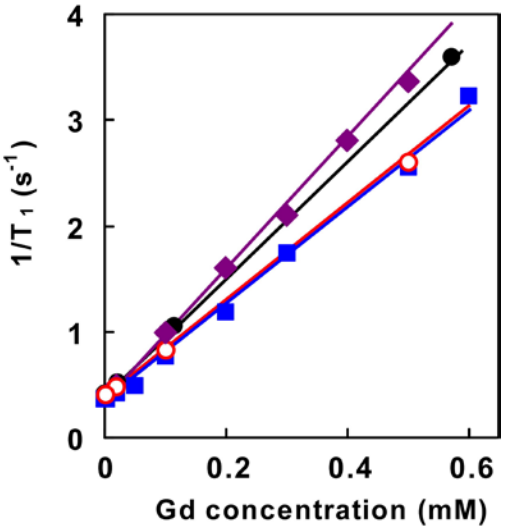

Figure 4. Plots of $1/T_1$ for Gd-DOTA (open circles), G1-DL-DOTA-Gd (squares), G3-DL-DOTA-Gd (diamonds), and G3-DL-DOTA-Gd-incorporated liposome (circles) as a function of Gd^{3+} concentration. Longitudinal relaxivities of Gd-DOTA, G1-DL-DOTA-Gd, G3-DL-DOTA-Gd, and G3-DL-DOTA-Gd-incorporated liposome are evaluated to be 4.6, 4.6, 6.2 and 5.5 ($mM^{-1}s^{-1}$).

3.3. In vivo MR imaging of copoly(EOEOVE-block-ODVE)-modified liposomes containing Gd-DOTA-dendron-based lipids

Detection of the Gd-DOTA-incorporated liposomes in vivo using MRI was examined. Two kinds of the liposomes consisting of EYPC, Chol, PEG5000-PE, copoly(EOEOVE-block-ODVE, and G3-DL-DOTA-Gd at the mol ratio of 42/42/4/2/10 with average diameters of 110 and 48 nm were prepared by the extrusion method using membranes with a pore size of 100 nm or 50 nm. These liposomes were administrated intravenously to BALB/c nude mouse having colon 26 tumor of about 200 mm^3 from tail vein and the accumulation of the liposomes at the tumor was monitored with MRI. Figures 5 A-D depict

the MR images of the tumor before (A) and at 1 h (B), 3 h (C), 8 h (D) after the liposome with an average diameter of 110 nm. Apparently, MR signal at the tumor site increased with time, indicating that the amount of the liposomes accumulating at the tumor site increased with time. Similar increase in MR signal intensity was observed for the tumor-bearing mouse administered with the G3-DL-DOTA-Gd containing liposomes with an average diameter of 48 nm (Figures 5 E-H). These liposomes provided MR images with high resolution as is obvious in Figures 5 A-H. Therefore, they revealed that the liposomes did not distribute homogenously in the tumor site: the areas with high liposome accumulation and those with poor liposome accumulation coexist in the tumor sites, which might be reflected from local disparity in the tumor tissue composition, tissue anatomy and vascularization [42,43]

We attempted to detect difference in the tumor accumulation efficiency between these liposomes using MRI. Because MR images of these liposomes were taken using different mice, their MR signal intensities were normalized to those of muscle, where distribution of liposomes might be negligible, for each mouse. Figure 5 I showed the time courses of area-averaged MR signal intensities at the tumor site of the liposome-injected mice. In both cases, the signal intensity increased with time and reached a constant revel at 8 h after the liposome injection, suggesting that these liposomes accumulated at the tumor in a similarly time-dependent manner irrespective of the liposome diameter difference. However, when signal intensity values at the tumor sites at the same time point between these liposome-injected mice, the tumor of the mouse injected with the larger liposomes exhibited

stronger signal intensity. This result suggests that the liposomes with 110 nm diameter accumulated at the tumor more efficiently that those with 48 nm diameter.

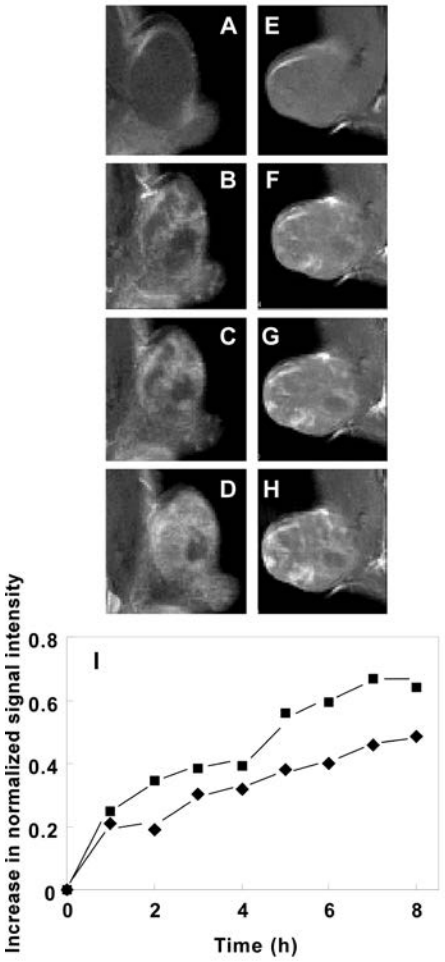

Figure 5. Tumor accumulation of liposomes with average diameters of 110 nm (A-D) and 48 nm (E-H). MR images of tumors before (A,E) and 1h (B,F), 3h (C,G), and 8h (D,H) after administration of liposomes. (I) Plots of increase in the area averaged MR signal intensity for tumor of BALB/c nude mouse injected with liposome of 110 nm (squares) or 48 nm (diamonds) as a function of time. Tumor sizes shown in A and E were 193 and 204 mm^3, respectively. MR signal intensities of tumors were normalized by MR signal intensities of muscle of each mouse.

We further attempted to detect difference in the tumor accumulation efficiency between two tumors of different sizes in the same mouse. Figures 6 A and B displayed MR images of

tumor sites with volumes of 141 mm^3 (left side) and 242 mm^3 (right side) before and 8 h after intravenous administration of the liposomes. After the liposome administration, MR signal intensity apparently increased at both tumors, indicating that the liposomes were distributed in both tumor sites. To compare accumulation efficiency of the liposomes between these tumors, the area-averaged signal intensities of these tumor sites were plotted against various time points (Figure 6 C). Signal intensities of at these tumor sites increased with time and reach a

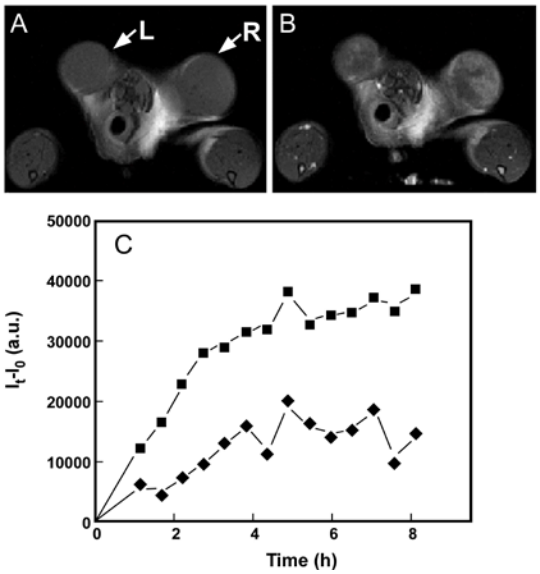

Figure 6. Influence of tumor size on liposome accumulation. MRIs of left (L) and right (R) tumors before (A) and 8 h after (B) liposome administration. (C) Plots of increase in MR signal intensity of left (diamonds) and right (squares) tumors as a function of time. Sizes of left and right tumors were 141 and 242 mm^3, respectively. Liposomes with a diameter of 110 nm were used.

constant revel after around 8 h for the larger tumor or around 5 h for the smaller tumor. However, in comparison of signal intensities between these tumors, the larger tumor exhibited almost two fold higher accumulation of liposomes, as judged from their area-averaged MR signal intensities. It is known that liposomes with a diameter around 100 nm accumulate at

tumor site through the EPR effect [44,45] which is based on the enhanced permeability of blood vessels in the tumor tissues. Therefore, it seems likely that the larger tumor might contain more capillary vessels with higher permeability to the liposomes than the smaller tumor, resulting in more efficient accumulation of the liposomes at the larger tumor.

We also examined whether MR signal intensity at the tumor site is proportional to the amount of Gd^{3+} or not. The increase in reciprocal of T_1 is proportional to the increase in the concentration of Gd^{3+} ion. Therefore, the increase in MR signal intensity of the right tumor was plotted against the increase in the reciprocal of T_1 (Figure 7). Apparently, these plots are fit on a straight line, indicative of linear relationship between them. The result demonstrates

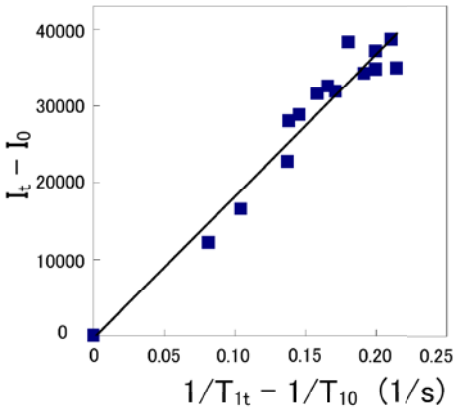

Figure 7 Plots of correlation between increase in inverse the relaxation time and increase in MR signal intensity of tumor (Tumor-R1 of Fig. 6).

that MR signal intensity at the tumor is proportional to Gd^{3+} ion concentration at the tumor site, and hence accumulation of the liposomes bearing Gd^{3+} ion can be accurately traced by following MR signals.

3.4. Tumor-specific DOX delivery by copoly(EOEOVE-block-ODVE)-modified pegylated

liposomes containing Gd-DOTA-dendron-based lipids

We examined influence of inclusion of G3-DL-DOTA-Gd on the drug encapsulation and release function of the copolymer-modified pegylated liposomes. Encapsulation efficiencies of DOX for the polymer modified pegylated liposomes with G3-DL-DOTA-Gd contents of 0, 5, and 10 mol% were estimated to be 95, 95 and 83 %, respectively. Inclusion of 5 mol% of the Gd-DOTA-dendron-based lipid did not affect DOX encapsulation, but lipid 10 mol% of the Gd-DOTA-dendron-based lipid slightly decreased encapsulation efficiency. Probably, higher content of the dendron-based lipid may disturb packing of the liposomal lipids slightly and decreased the pH gradient, which induce encapsulation of DOX in the liposome lumen during DOX loading procedure.

Figure 8 A shows time courses of DOX release from the liposomes with varying

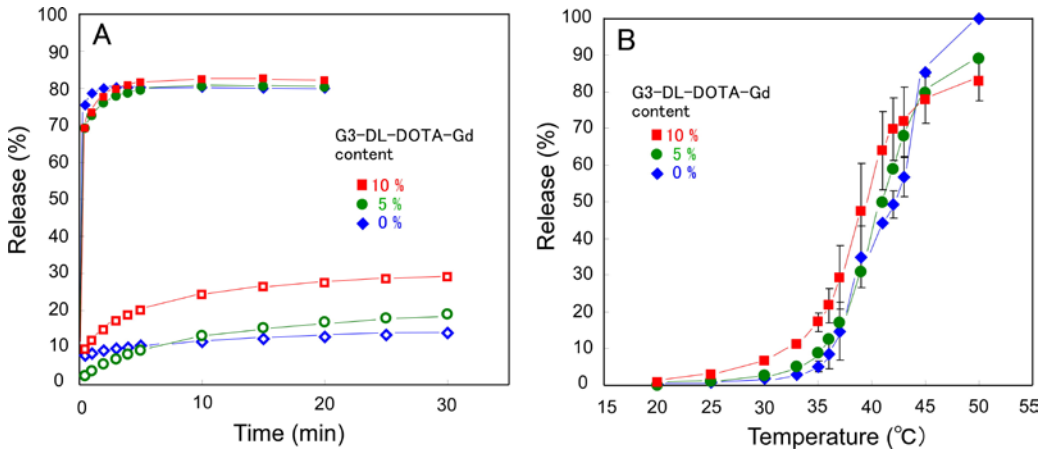

Figure 8. Doxorubicin release from temperature-sensitive liposome with varying G3-DL-DOTA-Gd contents in HBS containing 10 % FBS. (A) Time course at 36 °C (open symbols) or 45 °C (closed symbols). (B) Percent release after 10 min incubation.

G3-DL-DOTA-Gd contents. All liposomes exhibited low extents of DOX release at 36°C, but

their DOX release was significantly promoted at 45°C. Poly(EOEOVE) chains with transition temperature around 38 °C were hydrated and hardly interact with the liposome membrane at 36 °C. However, these polymer chains became dehydrated and strongly destabilized the membrane through hydrophobic interaction at 45°C [36,37]. For more detailed comparison of DOX release behaviors of these liposomes, their temperature-dependence of DOX release was shown in Figure 8B. Apparently, their DOX release was enhanced significantly above 37°C, which again indicates the participation of the transition of the polymer chains in the enhancement of DOX release. When compared with the case of the liposomes without G3-DL-DOTA-Gd, the liposomes with the G3-DL-DOTA-Gd content of 5% exhibited almost the same temperature-dependent DOX release property. The liposomes with the G3-DL-DOTA-Gd content of 10% showed slightly higher extent of DOX release between 25 and 43°C, suggesting that inclusion of too much content of G3-DL-DOTA-Gd may make the membrane slightly leakier. Probably, presence of the dendron-based lipid in the EYPC and Chol membranes might disturb ordered packing of the lipid molecules to some extent, but the influence on temperature-responsive release property of the liposomes is not remarkable.

Finally, we examined the performance of the copolymer-modified pegylated liposomes containing G3-DL-DOTA-Gd as drug delivery system for tumor-specific chemotherapy from the viewpoint of anti-tumor effect by the delivered drug. We used the copolymer-modified pegylated liposomes with G3-DL-DOTA-Gd content of 5% for this experiment because they showed excellent temperature-controlled DOX release behavior (Figure 8).

We prepared mice bearing tumors with volume of ca. 200 mm^3 by inoculating mouse colon carcinoma 26 cells into the right flank of BALB/c mice. The liposomes encapsulating DOX were injected intravenously via the tail vein. Because accumulation of the liposomes at the tumor tissue was shown to reach a constant level at around 8 h after their administration (Figures 5 and 6), the tumor site was locally heated at 44°C for 10 min at 8 h after the administration using a radio frequency oscillator as previously reported [37,39]. Control experiments were also done to the tumor-bearing mice with or without heating at 44°C for 10 min using the same procedure.

As depicted in Figure 9, the local heating at 44 °C for 10 min hardly affected tumor growth in comparison with the saline-injected mice without local heating. We have already reported that effect of local heating is at a negligible level, because the 10-min heating might be too short to generate the tumor-growth-suppressive effect of hyperthermia [37]. When the DOX-loaded liposomes were injected to the tumor-bearing mice and local hyperthermia was not applied, the tumor grew quite quickly as the mice that had been injected with saline. However, when the tumor site was heated at 44°C for 10 min, the tumor growth was strongly suppressed and tumor was even shrunk with time. Because the liposomes retained DOX in the inner space, those accumulating at the tumor might hardly affect its growth. However, when mild heating was applied to the tumor site, DOX molecules were immediately released from the liposomes and attacked to the tumor cells, resulting in shrinking of tumor volume.

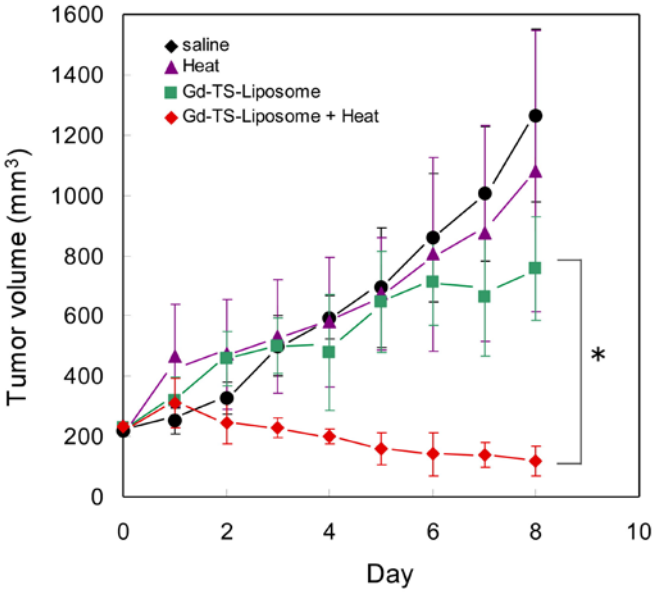

Figure 9. Time course of tumor growth after injection DOX-loaded liposomes with (diamonds) or without (squares) local heating. DOX dose was 6 mg/kg body weight. The data represent mean±S.D.(n=4). *, P<0.01. Injection of saline (HBS) without heating (circles) and heating without injection (triangles) were also performed as control experiments.

To date, various types of drug carriers having imaging functions have been designed. Some of these carriers work simply as “dual purpose systems” for both chemotherapy and diagnosis. However, multifunctional carriers having stimuli-responsive drug release and imaging functions have possibility to increase efficacy of chemotherapy, in which information of accumulation of the carriers at the target tissues can enhance bioavailability of drug through application of stimuli to the target sites at the best timing. Temperature-sensitive liposomes having imaging functions are most intensively studied from the practical viewpoint. For example, water soluble Gd-chelates [46] and Mn^{2+} [47-49] were loaded into lysolipid-based temperature-sensitive liposomes for quantification and monitoring of the drug release process in the target tissues. Because these liposomes were heated in the initial stage

of the liposome administration (0-15 min after the administration), the liposome distribution at the tumor was monitored in a short period of 90 min [47,48].

We have shown that the copoly(EOEOVE-*block*-ODVE)-modified pegylated DOX-loaded liposomes were stable at physiological temperature and hence they still retained the ability to attack strongly the tumor even after 12 h after their administration upon mild heating at the tumor [37]. Therefore, it is of importance to follow accumulation process of our liposomes for the long time period, which enables optimization of drug delivery to maximize therapeutic efficacy of drugs. Our liposomes having Gd-chelate-dendron-based lipid exhibited both the highly temperature-responsive drug release and the sensitive MR imaging functions. These multifunctional liposomes can provide information on the location of tumor sites and the accumulation process of liposomes at the tumor sites. Based on information, drug molecules can be released at the tumor sites by heating the tumor sites at the best timing, resulting in highly efficient therapeutic effect of drug. In addition, the imaging function of the liposomes can be used to optimize liposome characters, such as liposome compositions and liposome size, for better accumulation at the tumor sites through preliminary administration with the liposomes without drug. Indeed, characters of tumors should vary depending on individual patients, but the multifunctional liposomes might lead to an effective chemotherapy optimized to individual patient.

4. Conclusion

We developed a new type of multifunctional liposomes having temperature-responsive drug release and MR imaging functions by using a temperature-sensitive copoly(EOEOVE-block-ODVE) and newly synthesized Gd-chelate-attached dendron lipid. The liposomes provided MR image with high resolution and hence their accumulation process were able to be followed by MRI. The liposomes were stable at physiological temperatures, but exhibited a significant release of encapsulated doxorubicin (DOX) after mild heating. In addition, the liposomes encapsulating DOX injected intravenously into tumor-bearing mice strongly suppressed tumor growth only when the tumor site was heated to 44°C for 10 min at 8 h after injection. The multi-functional liposomes having temperature-triggered drug release and MRI functions may lead to personalized chemotherapy, which is optimized to individual patient.

Acknowledgments.

We thank Dr. Masayuki Yokoyama of The Jikei University School of Medicine, Sayaka Shibata of National Institute of Radiological Sciences, and Noriko Tano of Osaka Prefecture University for supports in synthesis of Gd-DOTA-based dendron lipids, animal preparation for *in vivo* MR imaging experiments and preparation of figures, respectively. This work was supported in part by a Grant-in-Aid for Research on Nanotechnical Medicine from the Ministry of Health, Labor and Welfare of Japan and by a Grant-in-aid for Scientific Research from the Ministry of Education, Science, Sports, and Culture in Japan.

References

1) Riehemann K, Schneider SW, Luger TA, Godin B, Ferrari M, Fuchs, H. Nanomediciene-Challenge and perspectives. Angew Chem Int Ed 2009;48:872-97.

2) Ferrari M. Cancer nanotechnology: opportunities and challenges. Nature Rev Cancer 2005;5:161-71.

3) LaVan DA, Lynn DM, Langer R. Moving smaller in drug discovery and delivery. Nat Rev Drug Discov 2002;1:77-84.

4) Maeda H, Wu J, Sawa T, Matsumura Y, Hori K. Tumor vascular permeability and the EPR effect in macromolecular therapeutics: a review. J Control Release 2000;65:271-84.

5) Dancan R. Polymer conjugates as anticancer nanomedicines. Nature Rev Cancer 2006;6:688-701.

6) Ganta S, Devalapally H, Shahiwala A, Amiji M. A review of stimuli-responsive nanocarriers for drug and gene delivery. J Control Release 2008;126:187-204.

7) Farokhzad OC, Langer R. Nanomedicine: developing smarter therapeutic and diagnostic modalities. Adv Drug Delivery Rev 2006;58:1456-9.

8) Weinstein, JN, Magin, RL, Yatvin MB, Zaharko, DS. Liposomes and local hyperthermia: selective delivery of methotrexate to heated tumors. Science 1979;204:188-91.

9) Portney NG, Ozkan M. Nano-oncology: drug delivery, imaging, and sensing. Anal Bioanal Chem 2006;384:620-30.

10) Dell DD, Gianolio E, Crich SG, Terreno E, Aime S. Metal containing nanosized systems for MR-molecular imaging applications. Coordination Chemistry Rev 2008;252:2424-43.

11) Liong M, Lu J, Kovochich M, Xia T, Rhehm S, Nel AE, Tamanoi F, Zink JI. Multifunctional inorganic nanoparticles for imaging, targeting, and drug delivery. ACS Nano 2008;2:889-96.

12) Sun C, Lee JSH, Zhang M. Magnetic nanoparticles in MR imaging and drug delivery. Adv Drug Delivery Rev 2008;60:1252-65.

13) Shiraishi K, Kawano K, Minowa T, Maitani Y, Yokoyama M. Preparation of in vivo imaging of PEG-poly(L-lysine)-based polymeric micelle MRI contrast agents. J Control Rel 2009;136:14-20.

14) Mulder WJM, Strijkers GJ, van Tilborg GAF, Griffioen AW, Nicolay K. Lipid-based nanoparticles for contrast-enhanced MRI and molecular imaging. NMR Biomed 2006;19:142-64.

15) Walther C, Meyer K, Rennert R, Neundorf, I. Quantum dot-carrier peptide conjugates suitable for imaging and delivery applications. Bioconj Chem 2008;19:2346-56.

16) Guo Y, Shi DL, Cho HS, Dong ZY, Kulkarni A, Pauletti GM, Wang W, Lian J, Liu W, Ren L, Zhang QQ, Liu GK, Huth C, Wang LM, Ewing RC, In vivo imaging and drug

strage by quantum-dot-conjugated carbon nanotubes. Adv Funct Mater 2008;18:2489-97.

17) Weng KC, Noble CO, Papahajopoulos-Sternberg B, Chen FF, Drummond DC, Kirpotin DB, Wang D, Hom YK, Hann B, Park JW. Targeted tumor cell internalization and imaging of multifunctional quantum dot-conjugated immunoliposomes in vitro and in vivo. Nano Lett 2008;2581-7.

18) Veiseh O, Gunn JW, Zhang M. Design and fabrication of magnetic nanoparticles for targeted drug delivery. Adv Drug Delivery Rev 2010;62:284-304.

19) Herth MM, Barz M, Moderegger D, Allmeroth M, Jahn M, Thews O, Zentel R, Rosch F. Radioactive labeling of defined HPMA-based polymeric structures using [^{18}F]FETos for in vivo imaging by positron emission tomography. Biomacromolecules 2009;10:1697-1703.

20) Urakami T, Akai S, Katayama Y, Harada N, Tsukada H, Oku N. Novel amphiphilic probes for [18F]-radiolabeling performed liposomes and determination of liposomal trafficking by positron emission tomography. J Med Chem 2007;50:6454-7.

21) Papahadjopoulos D, Jacobson K, Nir S, Isac T. Phase transitions in phospholipid vesicles: fluorescence polarization and permeability measurements concerning the effect of temperature and cholesterols. Biochim Biophys Acta 1973;311:330-48.

22) Yatvin MB, Weinstein JN, Dennis WH, Blumenthal R. Design of liposomes for enhanced local release of drugs by hyperthermia. Science 1978;202:1290-3.

23) Ellens H, Benz J, Szoka FC. pH-Induced destabilization of phosphatidylethanolamine-containing liposomes: role of bilayer contact, Biochemistry 1984;23:1532-8.

24) Needham D, Anyarambhatla G, Kong G, Dewhirst MW. A new temperature-sensitive liposome for use with mild hyperthermia: characterization and testing in a human tumor xenograft model. Cancer Res 2000;60:1197-201.

25) Kono K. Thermosensitive polymer-modified liposomes. Adv Drug Delivery Rev 2001;53:307-19.

26) Kono K, Hayashi H, Takagishi T. Temperature-sensitive liposomes: liposomes bearing poly(N-isopropylacrylamide). J Control Release 1994;30:69-75.

27) Kim JC, Bae SK, Kim JD. Temperature-sensitivity of liposomal lipid bilayers mixed with poly(N-isopropylacrylamide-co-acrylic acid). J Biochem (Tokyo) 1997;121:15-9.

28) Chandaroy P, Sen A, and Hui SW. Temperature-controlled content release from liposomes encapsulating Pluronic F127. J Control Release 2001;76:27-37.

29) Ringsdorf H, Sackmann E, Simon J, Winnik FM. Interactions of liposomes hydrophobically-modified poly(N-isopropylacrylamides): an attempt to model the cytoskeleton. Biochim Biophys Acta 1993;1153:335-44.

30) Yoshino K, Kadowaki A, Takagishi T, Kono K. Temperature-sensitization of liposomes by use of N-isopropylacrylamide copolymers with varying transition endotherms. Bioconjug Chem 2004;15:1102-9.

31) Ta T, Convertine AJ, Reyes CR, Stayton PS, Porter TM. Thermosensitive liposomes modified with poly(N-isopropylacrylamide-co-propylacrylic acid) copolymers for triggered release of doxorubicin. Biomacromolecules 2010;11:1915-20.

32) Tilcock C, Ahkong QF, Koenig SH, Brown RD III, Davis M, Kabalka G. The design of liposomal paramagnetic MR agents: effect of vesicle size upon the relaxivity of surface-incorporated lipophilic chelates. Magn Reson Med 1992;27:44-51.

33) Kabalka GW, Davis MA, Holmberg E, Maruyama K, Huang L. Gadolinium-labeled liposomes containing amphiphilic Gd-DTPA derivatives of varying chain length: targeted MRI contrast enhancement agents for the liver. Magn Reson Imaging 1991;9:373-7.

34) Weissig V, Babich J, Torchilin V. Long-circulating gadolinium-loaded liposomes: potential use for magnetic resonance imaging of the blood pool. Colloid Surf B: Biointerfaces 2000;18:293-9.

35) Torchilin VP. Surface-modified liposomes in gamma- and MR-imaging. Adv Drug Delivery Rev 1997;24;301-13.

36) Kono K, Murakami T, Yoshida T, Haba Y, Kanaoka S, Takagishi T, et al. Temperature sensitization of liposomes by use of thermosensitive block copolymers synthesized by living cationic polymerization: effect of copolymer chain length. Bioconjugate Chem 2005;16:1367-74.

37) K. Kono, T. Ozawa, T. Yoshida, F. Ozaki, Y. Ishizaka, K. Maruyama, C.Kojima, A.

Harada, S. Aoshima, "Highly temperature-sensitive liposomes based on a thermosensitive block copolymer for tumor-specific chemotherapy", **Biomaterials**, **31**, 7096-105 (2010).

38) Takahashi T, Kojima C, Harada A, Kono K. Alkyl chain moieties of polyamidoamine dendron-bearing lipids influence their function as a nonviral gene vector. Bioconj Chem 2007;18:1349-54.

39) Maruyama K, Unezaki S, Takahashi N, Iwatsuru M. Enhanced delivery of doxorubicin to tumor by long-circulating thermosensitive liposomes and local hyperthermia. Biochim Biophys Acta 1993;1149:209-16.

40) Weigele M, De Bernardo SL, Tengi JP, Leimgruber W. Novel reagent for the fluorometric assay of primary amines. J Am Chem Soc 1972;94:5927-8.

41) Tóth É, Pubanz D, Vauthey S, Helm L, Merbach AE. The role of water exchange in attaining maximum relaxivities for dendrimeric MRI contrast agents. Chem Eur J 1996;2:1607-15.

42) Patterson EJ, Scudamore CH, Owen DA, Nagy AG, Buczkowski AK. Radiofrequency ablation of porcin liver in vivo: effects of blood flow and treatment time on lesion size. Ann Surg 1998;227:559-65.

43) Frich L, Bjornerud A, Fossheim S, Tillung T, Gladhaug I. Experimental application of thermosensitive paramagnetic liposomes for monitoring magnetic resonance imaging guided thermal alblation. Magn Reson Med 2004;52:1302-9.

44) Gabizon A, Papahadjopoulos D. Liposome formulations with prolonged circulation time in blood and enhanced uptake by tumors. Proc Natl Acad Sci USA 1988;85:6949-53.

45) Woodle M, Lasic DD. Sterically stabilized liposomes. Biochim Biophys Acta 1992;1113:171-99.

46) de Smet M, Langereis S, van den Bosch S, Grull H. Temperature-sensitive liposomes for doxorubicin delivery under MRI guidance. J Control Rel 2010;143:120-7.

47) Viglianti BL, Abraham SA, Michelich CR, Yarmolenko PS, MacFall JR, Bally MB, Dewhirst MW. In vivo monitoring of tissue pharmacokinetics of liposome/drug using MRI: illustration of targeted delivery. Magn Reson Med 2004;51:1153-62.

48) Ponce AM, Viglianti BL, Yu D, Yarmolenko PS, Micheloch CD, Woo J, Bally MB, Dewhirst MW. Magnetic resonance imaging of temperature-sensitive liposomes release: drug dose painting and antitumor effects. J Natl Cancer Inst 2007;99:53-63.

49) Viglianti BL, Ponce AM, Micheloch CD, Yu D, Abraham SA, Sanders L, Yarmolenko PS, Schroeder T, MacFall JR, Barboriak DP, Colvin M, Bally MB, Dewhirst MW. Chemodosimetry of in vivo tumor liposomal drug concentration using MRI. Magn Reson Med 2006;56:1011-8.